Experimental study on the estimation of lever arm in GPS/INS

Article *in* IEEE Transactions on Vehicular Technology · April 2006

DOI: 10.1109/TVT.2005.863411 · Source: IEEE Xplore

CITATIONS
52

READS
1,542

5 authors, including:

Sinpyo Hong
Pusan National University
29 PUBLICATIONS **456** CITATIONS
SEE PROFILE

Ho Hwan Chun
Pusan National University
211 PUBLICATIONS **2,371** CITATIONS
SEE PROFILE

Jason Speyer
University of California, Los Angeles
340 PUBLICATIONS **6,832** CITATIONS
SEE PROFILE

Experimental Study on the Estimation of Lever Arm in GPS/INS

Sinpyo Hong, Man Hyung Lee, *Senior Member, IEEE*, Ho-Hwan Chun, Sun-Hong Kwon, and Jason L. Speyer, *Life Fellow, IEEE*

***Abstract*—Lever-arm uncertainty can be an important error source in the integration of the Global Positioning System (GPS) and inertial navigation system (INS). This paper presents both numerical and experimental studies on the estimation of the lever arm in the integration of a very-low-grade inertial measurement unit (IMU) with an accurate single-antenna GPS measurement system. Covariance simulation results showed that maneuvers play an important role on the estimation of the lever arm and attitude. The length of the lever arm has a rather insignificant effect on the estimation of these. Experimental tests conducted with a low-cost microelectromechanical system (MEMS) IMU and a carrier-phase differential GPS (CDGPS) measurement system showed that the lever arm can be estimated with centimeter-level accuracy. The test results confirmed that angular motions and horizontal accelerations improve the estimates of the lever arm and yaw angle, respectively.**

***Index Terms*—Global positioning system (GPS), inertial measurement unit (IMU), inertial navigation, inertial navigation system (INS), lever arm, observability.**

I. Introduction

ONE interesting research area in the application of low-cost inertial sensors is the integration of an accurate real-time Global Positioning System (GPS) measurement system with a lower grade microelectromechanical system (MEMS) inertial measurement unit (IMU) [1]–[4]. This type of GPS/IMU system is usually used for precise measurement in land or aerial navigation systems [5]–[10]. There are several advantages in this type of integration. First, a low-cost MEMS IMU that has compact size is readily available. Second, GPS measurement systems usually provide data at 1–10 Hz. With aid from GPS, an inertial navigation system (INS) does not need an expensive and accurate IMU in areas with open sky. Third, IMU can help resolving integer ambiguity or tracking of carrier phase in carrier-phase differential GPS (CDGPS). Fourth, a compact MEMS IMU is very useful for the applications that require small navigation systems. Last, single-antenna GPS measurement systems are simple, less expensive, and widely used compared with multiantenna systems.

As mentioned in [11], one of the major sources of error in accurate GPS/INS systems is the lever arm, the relative position of the GPS antenna with respect to the inertial sensor. The lever-arm error in large vehicles can be much greater than the positioning accuracy of CDGPS. Another important error source in the integration of low-grade IMU with the single-antenna GPS measurement system is yaw angle [11]–[13]. Yaw-angle error can introduce a large position error if the length of the lever arm is large [13]. In contrast to a multiantenna GPS measurement system, yaw error can increase relatively fast with time. The error growth rate is proportional to the error in the estimate of the vertical component of gyro bias. However, these errors that are unobservable with low dynamics can be made observable with time-varying motions [11].

Even though the lever arm was recently known to be made observable with rotational motions and the software to estimate the lever arm was developed by commercial vendors, rigorous research papers on the topic were published rarely [11], [14]–[16]. The main purpose of this paper is to experimentally confirm the theoretical results regarding the observability of the lever arm and attitude with position measurements. Special attention is given to the effect of the transient motions of a vehicle on the estimation of the lever arm and yaw angle. Even though the effect of acceleration changes on the estimation of INS errors were well studied [17]–[21], that of angular motion is not yet fully known. Due to many uncertainties in the statistics of sensor noises and dynamics of vehicles, the numerical simulation in [11] regarding the errors in the estimates of lever arm and attitude may not provide sufficient information about the estimator performance in real systems. Another purpose of the paper is to evaluate estimator performance in the integrated system of a single-antenna CDGPS and low-grade MEMS IMU based on experiments.

There are many practical questions related to the estimation of lever arm and yaw angle. Some of them can be as follows: Is it desirable to make the lever arm long for its estimation? How do the vehicle motions or GPS measurement noises affect the estimation? There have been several researches on these topics. The relation between the lever-arm length and yaw estimation was considered in [3] and [22]. The effect of vehicle motion on the error estimation was investigated with observability analysis

Manuscript received March 3, 2004; revised November 18, 2004, June 29, 2005, and August 16, 2005. This work was supported by the Korea Science and Engineering Foundation (KOSEF) through the Advanced Ship Engineering Research Center (ASERC) at Pusan National University. The review of this paper was coordinated by Dr. R. Klukas.

S. Hong is with the Advanced Ship Engineering Research Center (ASERC), Pusan National University, Changjeon-dong, Kumjeong-gu, Busan 609-735, Korea (e-mail: sinpyo@pusan.ac.kr).

M. H. Lee is with the School of Mechanical Engineering, Pusan National University, Busan 609-735, Korea.

H.-H. Chun is with the Department of Naval Architecture and Ocean Engineering, Pusan National University, Busan 609-735, Korea.

S.-H. Kwon is with the Department of Naval Architecture and Ocean Engineering, Pusan National University, Busan 609-735, Korea. He is also with the Department of Civil Engineering, Texas A&M University, College Station, TX 77843-3136 USA.

J. L. Speyer is with the Mechanical and Aerospace Engineering Department, University of California, Los Angeles, CA 90095-1597 USA.

Digital Object Identifier 10.1109/TVT.2005.863411

in [11]. In this paper, a more comprehensive and detailed study was conducted on these topics. Before test results are introduced, covariance simulation results on the error estimation are presented with various simulation conditions on vehicle motions, lever-arm length, initial estimation errors, and GPS-measurement-noise intensity.

Simulation results showed that the estimates of error states in GPS/INS integration can be improved significantly with fast vehicle maneuverings. The influence of lever-arm size and initial estimation error on the estimation of attitude and lever arm can be rather insignificant. However, a long lever arm may induce a large position error. Thus, for a vehicle that is capable of maneuvering with rapid changes in the motions of translation and rotation, a short lever arm may be desirable.

Three tests were conducted for the estimation of errors in the integrated system of GPS and INS. In each of the tests, a GPS antenna for position measurement and an IMU were mounted on a plate so that the relative position between the antenna and IMU can be accurately measured. Four GPS antennas were also mounted on the plate for attitude measurement to evaluate the accuracy of the attitude estimate. In the first test, the plate on which the GPS antennas and IMU were placed was shaken by hand repeatedly. The plate experienced large and fast angular motions. However, changes in position and acceleration were small. In the remaining two tests, the plate was fixed on the roof of a car. In the first car test, the car ran over an acrobatic path so that the car experienced motions of six degrees of freedom. In contrast to the table test, the car underwent relatively large acceleration changes and small attitude changes. In the second car test, the car ran over a wide flat ground with relatively slow changes in both angular and translatory motions.

Test results showed that angular motions of a vehicle improved the estimation of the lever arm. The direction of estimation improvement was orthogonal to the axis of rotation. In the manual table test, the estimation error was of centimeter level. However, the errors in the car tests were much greater than that of the manual table test. Test results also showed that acceleration changes in the horizontal plane improved the estimation of yaw angle. Root mean square (RMS) of the difference between the estimate and measurement of yaw was less than 1° in the first car test and greater than 2° in the manual table test and the second car test.

The error model and its observability properties in the GPS/INS system are briefly given in Section II. Covariance simulation results on error estimation for various test conditions are given in Section III. Measurement systems and test results are given in Sections IV and V, respectively. Conclusions are given in Section VI. Throughout this paper, notations for nomenclature and definitions of coordinate frames in [11] are used.

II. Error Model

This section briefly introduces the basic formulations for errors and their observability properties in GPS/INS integrations. First, error models for the integration of an accurate single-antenna GPS measurement system with low-grade IMU are introduced. The behavior of static estimation error is also given next. Information on static estimation error can be helpful for interpreting the results of simulations and tests given in Sections III and V, respectively. The earth-centered earth-fixed (ECEF) frame is the reference frame for the INS and GPS integration. Observability properties of the errors are discussed later in this section. The effect of lever-arm length as well as vehicle maneuvering on the error estimation is considered.

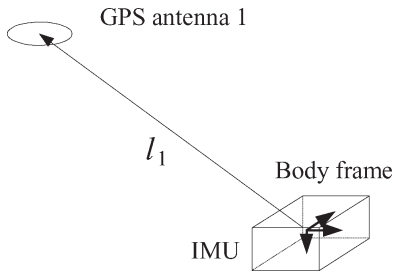

Fig. 1. Diagram of a GPS/INS sensor system.

The INS mechanization errors can be modeled as in [11], [15], and [16]

$$\dot{x} = Ax \tag{1}$$

with

$$x = \left[(\delta P^{\mathrm{e}})^{\mathrm{T}} \quad (\delta V^{\mathrm{e}})^{\mathrm{T}} \quad (\gamma^{\mathrm{b}})^{\mathrm{T}} \quad (\varepsilon_{\mathrm{g}})^{\mathrm{T}} \quad (\varepsilon_{\mathrm{a}})^{\mathrm{T}} \quad (\delta l)^{\mathrm{T}} \right]^{\mathrm{T}} \tag{2}$$

$$A = \begin{bmatrix} 0 & I_3 & 0 & 0 & 0 & 0 \\ 0 & 0 & -R_{\mathrm{b}}^{\mathrm{e}} F^{\mathrm{b}} & 0 & R_{\mathrm{b}}^{\mathrm{e}} & 0 \\ 0 & 0 & -\Omega_{\mathrm{eb}}^{\mathrm{b}} & I_3 & 0 & 0 \\ 0 & 0 & 0 & 0 & 0 & 0 \\ 0 & 0 & 0 & 0 & 0 & 0 \\ 0 & 0 & 0 & 0 & 0 & 0 \end{bmatrix} \tag{3}$$

where δP^{e} and δV^{e} are the ECEF frame representations of the position and velocity estimation errors, respectively; γ^{b}, ε_{g}, ε_{a}, and δl are the body-frame representations of the estimation errors of attitude, gyro bias, accelerometer bias, and lever arm; I_3 is the three-dimensional identity matrix; $R_{\mathrm{b}}^{\mathrm{e}}$ is the rotation matrix from the body frame to the ECEF frame; F^{b} is the cross-product matrix of the specific force vector f^{b}; and $\Omega_{\mathrm{eb}}^{\mathrm{b}}$ is the cross-product matrix of the vector $\omega_{\mathrm{eb}}^{\mathrm{b}}$, the body-frame representation of the angular velocity of the body frame with respect to the ECEF frame.

Fig. 1 shows the GPS/INS sensor system. The IMU is usually placed inside of a vehicle while the GPS antenna is mounted on the outside of the vehicle. The estimation error for the GPS measurement can be written as [11]

$$y = Cx \tag{4}$$

with

$$C = \begin{bmatrix} I_3 & 0 & -R_{\mathrm{b}}^{\mathrm{e}} L_1^{\mathrm{b}} & 0 & 0 & R_{\mathrm{b}}^{\mathrm{e}} \end{bmatrix} \tag{5}$$

where L_1^{b} is the cross-product matrix of l_1^{b}, which is the body-frame representation of the lever arm.

If the vehicle is motionless with small roll and pitch angles, attitude error and accelerometer bias satisfy the relation

$f^{\mathrm{b}} \times \gamma^{\mathrm{b}} \simeq \varepsilon_{\mathrm{a}}$. Thus, the static attitude error resulting from the accelerometer bias is

$$\gamma_x \simeq \frac{\varepsilon_{\mathrm{a}y}}{g}, \quad \gamma_y \simeq \frac{-\varepsilon_{\mathrm{a}x}}{g} \tag{6}$$

with

$$\gamma^{\mathrm{b}} = [\gamma_x \quad \gamma_y \quad \gamma_z]^{\mathrm{T}}, \quad \varepsilon_{\mathrm{a}} = [\varepsilon_{\mathrm{a}x} \quad \varepsilon_{\mathrm{a}y} \quad \varepsilon_{\mathrm{a}z}]^{\mathrm{T}} \tag{7}$$

where g is the normal gravity. However, since the horizontal components of specific force are very small, $|\gamma_z|$ becomes much larger than $|\gamma_x|$ and $|\gamma_y|$, and $|\varepsilon_{\mathrm{a}z}|$ becomes much smaller than $|\varepsilon_{\mathrm{a}x}|$ and $|\varepsilon_{\mathrm{a}y}|$.

The effect of vehicle motions on the error observability is briefly introduced in the following. Let $x_{\mathrm{u}}(= [(\delta P_{\mathrm{u}}^{\mathrm{e}})^{\mathrm{T}} \quad (\delta V_{\mathrm{u}}^{\mathrm{e}})^{\mathrm{T}} \quad (\gamma_{\mathrm{u}}^{\mathrm{b}})^{\mathrm{T}} \quad \varepsilon_{\mathrm{gu}}^{\mathrm{T}} \quad \varepsilon_{\mathrm{au}}^{\mathrm{T}} \quad \delta l_{\mathrm{u}}^{\mathrm{T}}]^{\mathrm{T}})$ be an unobservable mode of the system (A, C). Then, the measurement and all orders of time derivatives of it become zero vector such that [11]

$$y = \delta P_{\mathrm{u}}^{\mathrm{e}} - R_{\mathrm{b}}^{\mathrm{e}} L_1^{\mathrm{b}} \gamma_{\mathrm{u}}^{\mathrm{b}} + R_{\mathrm{b}}^{\mathrm{e}} \delta l_{\mathrm{u}} = 0 \tag{8}$$

$$\overset{(k)}{y} = 0, \qquad k = 1, 2, \ldots n-1. \tag{9}$$

The condition $\overset{(k)}{y} = 0$, for $k = 0, 1, 2$, is always satisfied with

$$\delta P_{\mathrm{u}}^{\mathrm{e}} = R_{\mathrm{b}}^{\mathrm{e}} L_1^{\mathrm{b}} \gamma_{\mathrm{u}}^{\mathrm{b}} - R_{\mathrm{b}}^{\mathrm{e}} \delta l_{\mathrm{u}} \tag{10}$$

$$\begin{aligned} \delta V_{\mathrm{u}}^{\mathrm{e}} = & -R_{\mathrm{b}}^{\mathrm{e}} \left(L_1^{\mathrm{b}} \Omega_{\mathrm{eb}}^{\mathrm{b}} - \Omega_{\mathrm{eb}}^{\mathrm{b}} L_1^{\mathrm{b}} \right) \gamma_{\mathrm{u}}^{\mathrm{b}} \\ & + R_{\mathrm{b}}^{\mathrm{e}} L_1^{\mathrm{b}} \varepsilon_{\mathrm{gu}} - R_{\mathrm{b}}^{\mathrm{e}} \Omega_{\mathrm{eb}}^{\mathrm{b}} \delta l_{\mathrm{u}} \end{aligned} \tag{11}$$

$$\varepsilon_{\mathrm{au}} = -\left(c_{\gamma,2} \gamma_{\mathrm{u}}^{\mathrm{b}} + c_{g,2} \varepsilon_{\mathrm{gu}} + c_{l,2} \delta l_{\mathrm{u}} \right) \tag{12}$$

where

$$c_{g,2} = L_1^{\mathrm{b}} \Omega_{\mathrm{eb}}^{\mathrm{b}} - 2\Omega_{\mathrm{eb}}^{\mathrm{b}} L_1^{\mathrm{b}} \tag{13}$$

$$c_{l,2} = \left(\Omega_{\mathrm{eb}}^{\mathrm{b}} \right)^2 + \dot{\Omega}_{\mathrm{eb}}^{\mathrm{b}} \tag{14}$$

$$c_{\gamma,2} = -F^{\mathrm{b}} - c_{g,2} \Omega_{\mathrm{eb}}^{\mathrm{b}} - c_{l,2} L_1^{\mathrm{b}} + L_1^{\mathrm{b}} \dot{\Omega}_{\mathrm{eb}}^{\mathrm{b}}. \tag{15}$$

The condition $\overset{(k)}{y} = 0$, for $k = 3, 4, \ldots, n-1$, can be expressed with

$$\mathbb{C} z = 0 \tag{16}$$

where

$$\mathbb{C} = \begin{bmatrix} c_{\gamma,3} & c_{g,3} & c_{l,3} \\ c_{\gamma,4} & c_{g,4} & c_{l,4} \\ \vdots & \vdots & \vdots \\ c_{\gamma,n-1} & c_{g,n-1} & c_{l,n-1} \end{bmatrix} \tag{17}$$

$$z = \left[\left(\gamma_{\mathrm{u}}^{\mathrm{b}} \right)^{\mathrm{T}} \quad \varepsilon_{\mathrm{gu}}^{\mathrm{T}} \quad \delta l_{\mathrm{u}}^{\mathrm{T}} \right]^{\mathrm{T}} \tag{18}$$

with

$$c_{\gamma,j+1} = \dot{c}_{\gamma,j} - c_{\gamma,j} \Omega_{\mathrm{eb}}^{\mathrm{b}} \tag{19}$$

$$c_{g,j+1} = \dot{c}_{g,j} + c_{\gamma,j} \tag{20}$$

$$c_{l,j+1} = \dot{c}_{l,j} \tag{21}$$

for $j = 2, 3, \ldots, n-2$. Thus, the observability of the GPS/INS system is determined by $\mathbb{C}$. If it has a full column rank, then the system is observable, and $x_{\mathrm{u}} = 0$.

Note that while $c_{\gamma,i}$ and $c_{g,i}$, for $i = 3, 4, \ldots, n-1$, are determined by l_1^{b}, f^{b}, $\omega_{\mathrm{eb}}^{\mathrm{b}}$, and their time derivatives, $c_{l,i}$, for $i = 3, 4, \ldots, n-1$, is determined by only $\omega_{\mathrm{eb}}^{\mathrm{b}}$ and its time derivatives. Thus, rotational motions directly influence the estimation of the lever arm. The length of the lever arm may not be an important factor in the lever-arm estimation. In $c_{\gamma,i}$ and $c_{g,i}$, for $i = 3, 4, \ldots, n-1$, l_1^{b} has linear forms, while $\omega_{\mathrm{eb}}^{\mathrm{b}}$ and its time derivatives have higher order nonlinear forms. Moreover, the specific force is combined with angular velocity and its time derivatives. Thus, the estimation of attitude, gyro bias, and lever arm can be much sensitive to rotational motions. It is interesting to note that when the vehicle experiences only acceleration motion, $c_{l,i}$, for $i = 3, 4, \ldots, n-1$ is 0. In this case, lever-arm error has no influence in the estimation of attitude and gyro bias.

III. Numerical Simulations

As shown in the previous section, estimation of error states can be influenced by several factors such as lever arm and vehicle motions. In addition to these factors, errors both in the initial estimates and in measurements also have influence on the error estimation. The effects of these various factors on the error estimation were investigated by the covariance simulations in this section. The simulation results in this section can be used as supplements to the experimental study on the lever-arm estimation given in later sections. Since errors in the estimates of attitude, gyro bias, and lever arm determine other unobservable errors, only these errors will be considered in the covariance simulations.

In order to investigate the effect of vehicle motions on the error estimation, three types of motions were used in the simulations. Details of the motions are shown in Figs. 2–16. Relatively fast changes in both acceleration and rotational speed can be found in motion 1. In motion 2, angular velocities were smaller than those in motion 1. Initial forward acceleration was the same as that in motion 1. The following accelerations of motion 2 were smaller than those in motion 1. In motion 3, accelerations were small compared with those in motion 2. However, angular velocities in motions 2 and 3 were the same. Three lever arms were also used in the simulations to study the effect of lever-arm size on the error estimation. The dimensions of the lever arms 1–3 in the body frame were $[10 \ -10 \ 10]$, $[1 \ -1 \ 1]$, and $[0.1 \ -0.1 \ 0.1]$, in meters, respectively.

In the covariance simulations, INS mechanization differential equations were integrated with the IMU data at 100 Hz. The solution to the mechanization equations was corrected with an extended Kalman filter at 1 Hz using GPS position measurements. All the noises in measurements from GPS and IMU were assumed to be Gaussian white. The standard deviation (STD) of the noise in GPS position measurement in the tangential frame was [0.03 0.03 0.045], in meters. Bias and the STD of the accelerometer noise were $[0.04 \ -0.05 \ -0.1]$ and 0.01, in meters per second squared, respectively. The bias and the STD of the gyro noise were $[0.05 \ -0.09 \ -0.1]$ and 0.1, in degrees per second, respectively. Initial estimation errors in the

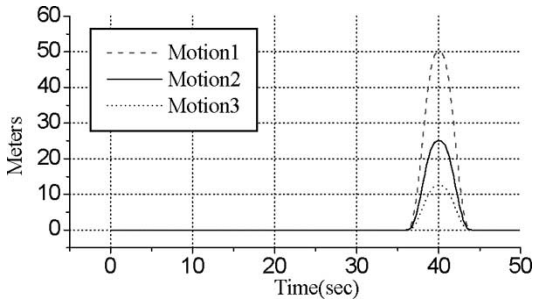

Fig. 2. Vehicle trajectory (east).

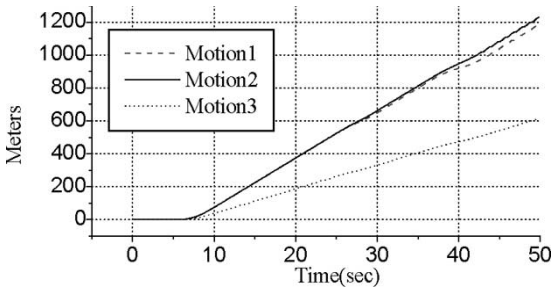

Fig. 3. Vehicle trajectory (north).

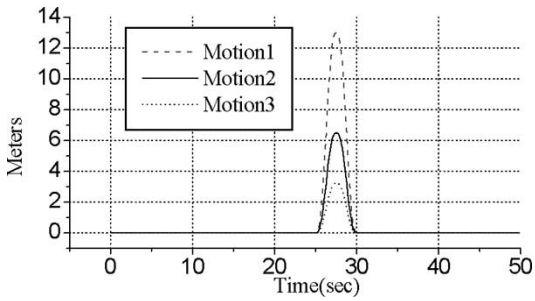

Fig. 4. Vehicle trajectory (up).

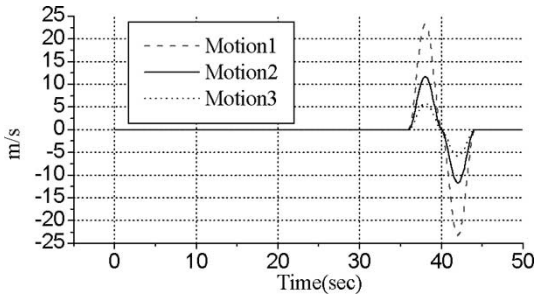

Fig. 5. Vehicle velocity (east).

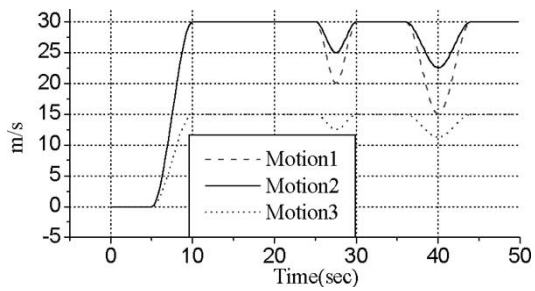

Fig. 6. Vehicle velocity (north).

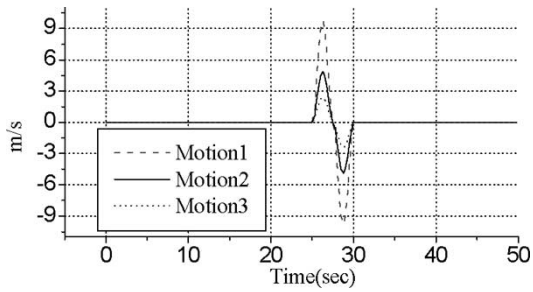

Fig. 7. Vehicle velocity (up).

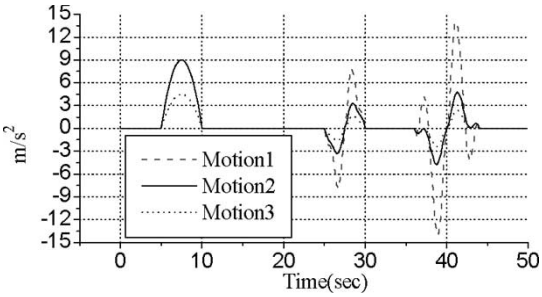

Fig. 8. Vehicle acceleration (forward).

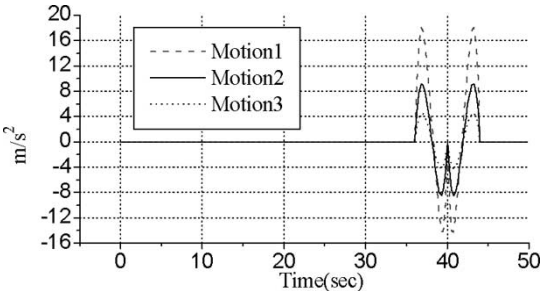

Fig. 9. Vehicle acceleration (right).

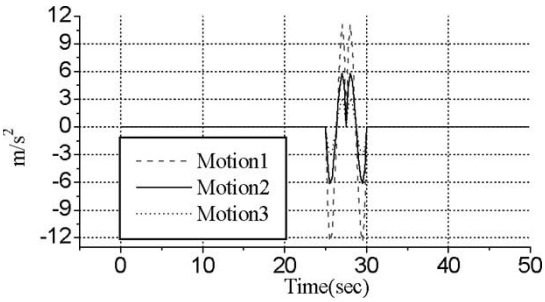

Fig. 10. Vehicle acceleration (down).

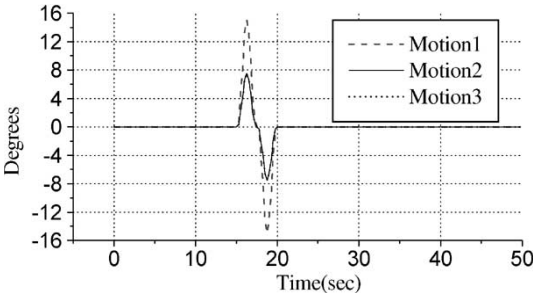

Fig. 11. Vehicle attitude (roll).

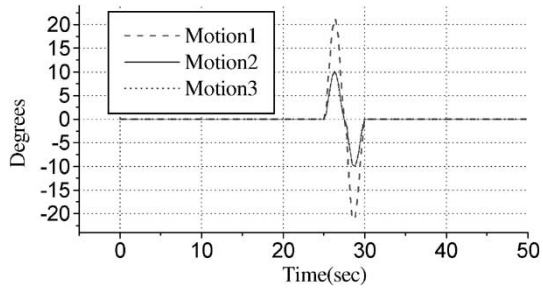

Fig. 12. Vehicle attitude (pitch).

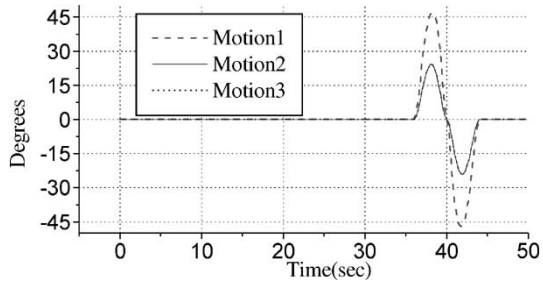

Fig. 13. Vehicle attitude (yaw).

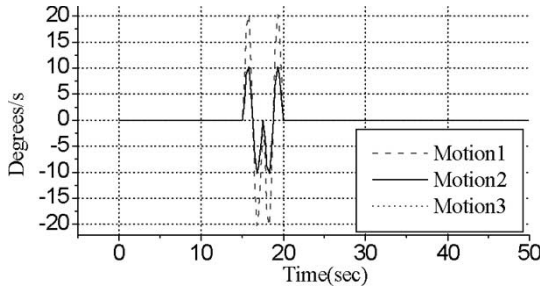

Fig. 14. Attitude rate (forward).

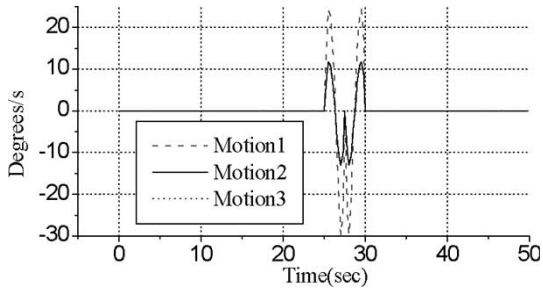

Fig. 15. Attitude rate (right).

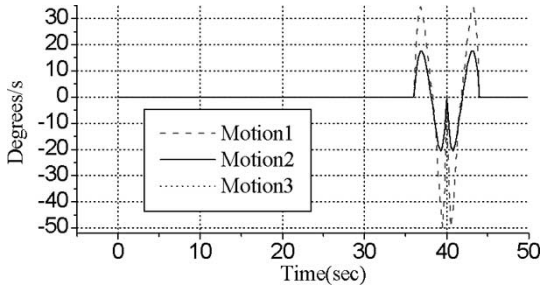

Fig. 16. Attitude rate (down).

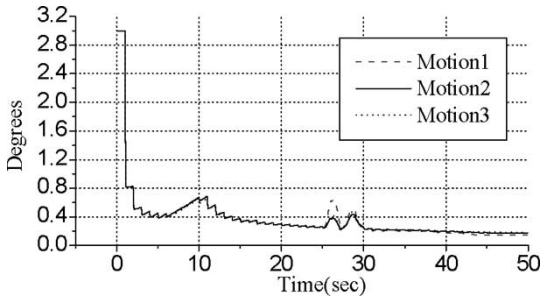

Fig. 17. STD of roll error with lever arm 2.

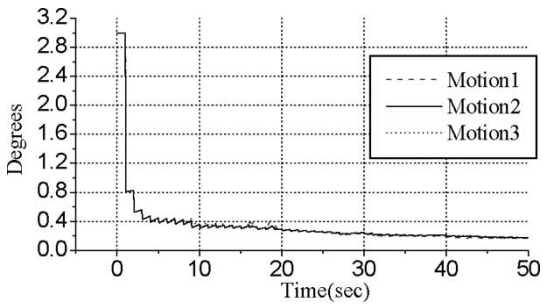

Fig. 18. STD of pitch error with lever arm 2.

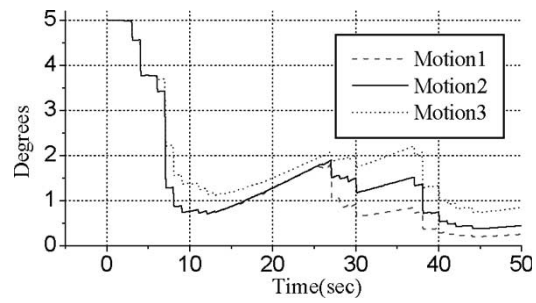

Fig. 19. STD of yaw error with lever arm 2.

simulations were as follows: Lever-arm error in the body frame was $[1\ 1\ -1]$ in meters, and attitude errors for roll, pitch, and yaw in degrees were 3, -3, and -5, respectively. Accelerometer bias error in the body frames was $-[0.04\ -0.05\ -0.1]$, in meters per second squared. Gyro-bias error in the body frame was $-[0.05\ -0.09\ -0.1]$, in degrees per second.

STDs of the estimation errors for the three motions are given in Figs. 17–25. These results were obtained from the simulation with lever arm 2. Except for the horizontal components of attitude and gyro bias, estimation results were shown to be sensitive to the motion of the vehicle. Figs. 19 and 22 show that there were large improvements in the estimates of the vertical components of attitude and gyro bias when the vehicle experienced acceleration changes. The best improvement was obtained with motion 1. Figs. 23–25 show that major changes in the estimates of lever arm were found when the angular velocity of the vehicle changed. Time responses for motions 2 and 3 are very similar and are quite different from that for motion 1. This implies that the estimation of lever arm is much sensitive to changes in angular velocity compared with those in acceleration.

STDs of the estimation errors for the three lever arms are also given in Figs. 26–34 for motion 2. From the figures, it

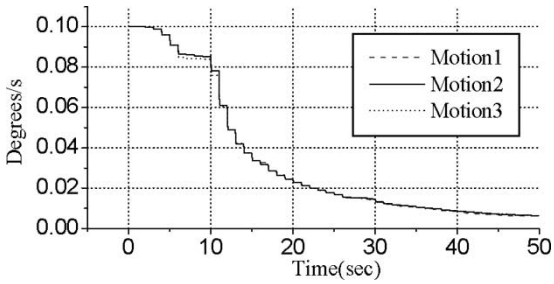

Fig. 20. STD of gyro-bias error with lever arm 2 (forward).

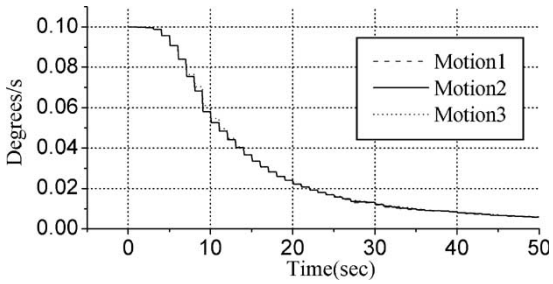

Fig. 21. STD of gyro-bias error with lever arm 2 (right).

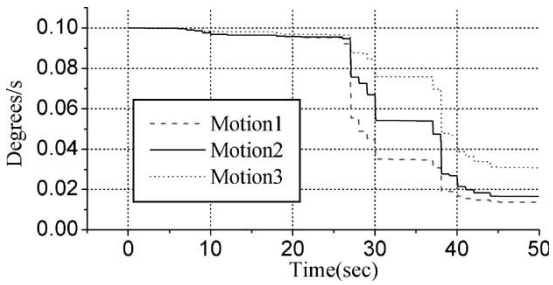

Fig. 22. STD of gyro-bias error with lever arm 2 (down).

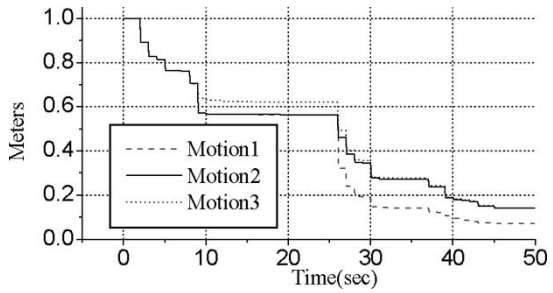

Fig. 23. STD of estimation error of lever arm 2 (forward).

can be seen that time responses of the estimation errors were generally quite insensitive to the changes in the lever-arm length. The length of the lever arm has almost no influence on the estimation results during the final time period of the simulations. Figs. 28 and 31 show that errors in estimates of the vertical components of attitude and gyro bias for lever arm 1 were small compared with those for lever arms 2 and 3 for the considerable part of the simulation time. However, the final values of the errors for all the three lever arms were almost the same.

Long lever arms are usually helpful in improving attitude estimation. The lever-arm effect can be seen clearly for rotational

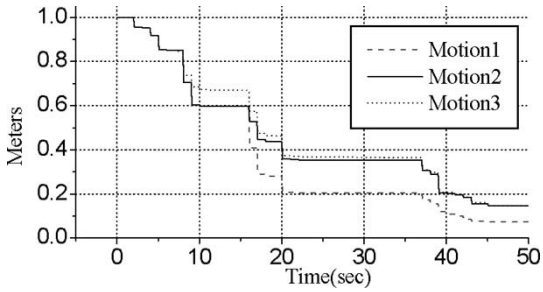

Fig. 24. STD of estimation error of lever arm 2 (right).

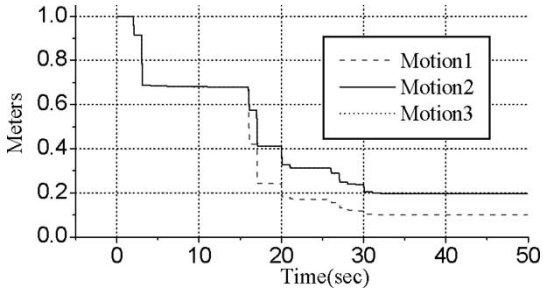

Fig. 25. STD of estimation error of lever arm 2 (down).

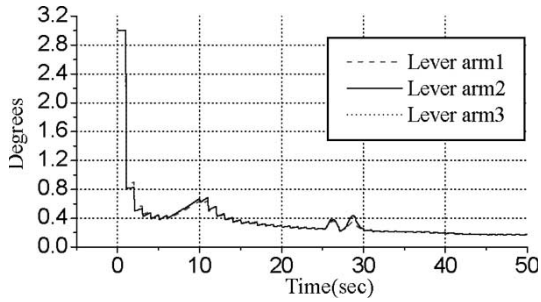

Fig. 26. STD of roll error with motion 2.

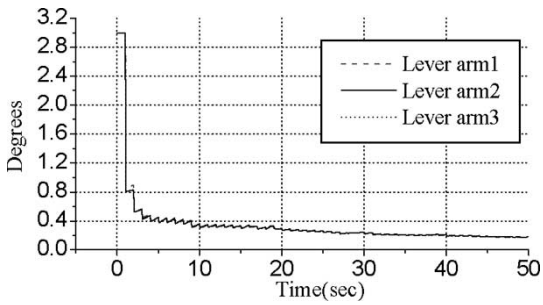

Fig. 27. STD of pitch error with motion 2.

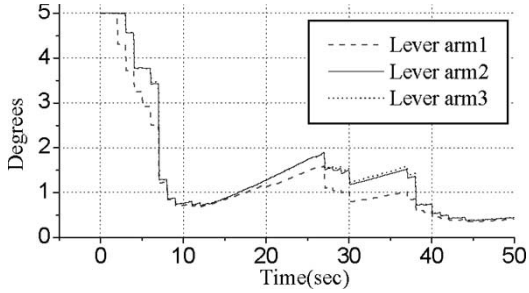

Fig. 28. STD of yaw error with motion 2.

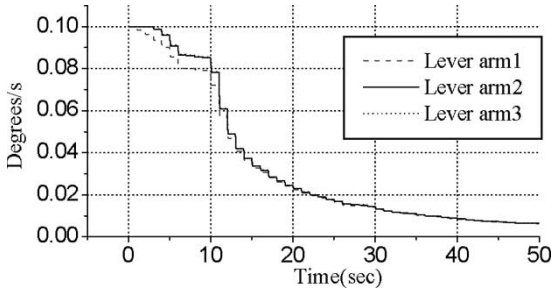

Fig. 29. STD of gyro-bias error with motion 2 (forward).

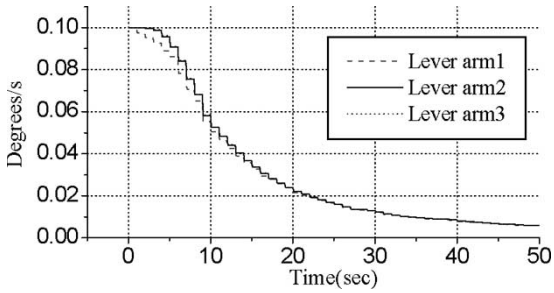

Fig. 30. STD of gyro-bias error with motion 2 (right).

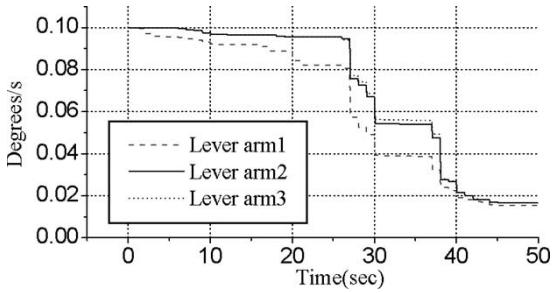

Fig. 31. STD of gyro-bias error with motion 2 (down).

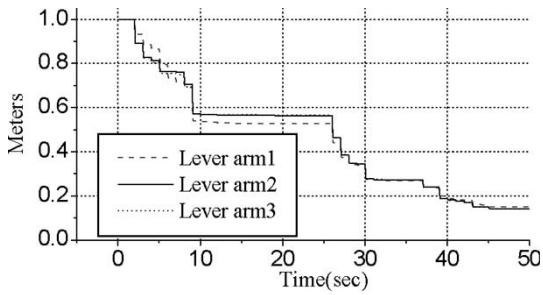

Fig. 32. STD of lever-arm error with motion 2 (forward).

motion with no translational velocity [3]. In the covariance simulation for the vehicle that rotates about the vertical axis through the accelerometer origin, the yaw error is shown to decrease as the length of the horizontal component of the lever arm increases. However, as stated in [11], changes in the specific force also improve the estimation of attitude. The results similar to Fig. 28 can be found in [22] on the effect of lever-arm length on the estimation of yaw angle. Comparison between errors in the estimate of yaw angle for the lever-arm lengths of 1 and 25 m are made in the covariance simulations with the motion of six degrees of freedom. Yaw error in the case

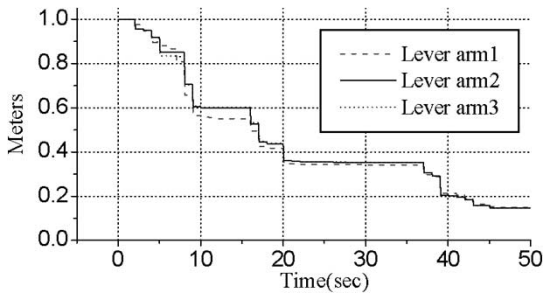

Fig. 33. STD of lever-arm error with motion 2 (right).

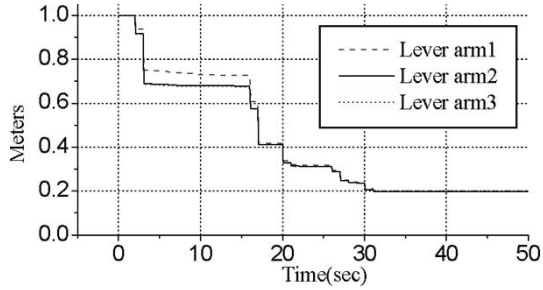

Fig. 34. STD of lever-arm error with motion 2 (Down).

of the lever arm of 25 m are shown to reach the same accuracy but with smaller and more even covariance.

In addition to the above numerical tests, other simulations with different GPS measurement noise and initial lever-arm estimation error were conducted. Final estimation errors in the above various situations are summarized in Table I. All the tests except tests 2 and 3 in the table were performed with the same sensor noises and initial state error that were given before in this section. Test conditions in test 2 are the same as those in test 1 except for initial lever-arm error. The initial lever-arm error in test 2 was twice as large as that in test 1. The table shows that the final estimation errors were little influenced by the initial error in the lever arm. Test conditions in test 3 were the same as those in test 1 except for GPS measurement noises. GPS measurement noises in test 3 were twice as large as that in test 1. The table shows that the lever-arm estimation was sensitive to the intensity of GPS measurement noise.

From the above covariance simulations, it can be seen that the estimates of the lever arm and attitude in GPS/INS integration are quite sensitive to vehicle motions. The influence of lever-arm size on the estimates is rather insignificant. It is well known that long lever arms cause a large position error [3], [22]. Thus, for a vehicle that is capable of maneuvering with rapid changes in the motions of translation and rotation, a long lever arm may not be desirable since the navigation system can have large position and velocity errors with little improvement in the estimation of other error states.

IV. Measurement Systems

This section introduces the measurement systems employed in the tests on the estimation of errors in the integrated navigation system of GPS and INS. Position measurements were obtained with dual-frequency CDGPS receivers. The measurement error in them was 1–2 cm. To verify the performance of

TABLE I
STDs OF ESTIMATION ERRORS AT THE FINAL SIMULATION TIME

Test types			Standard deviations of estimation errors								
No	Lever arm	Motion	Lever arm (m)			Attitude (deg)			Gyro Bias (deg/s)		
			F	R	D	R	P	Y	F	R	D
1	1	1	0.08	0.08	0.1	0.15	0.16	0.23	0.006	0.006	0.013
2†	1	1	0.08	0.08	0.1	0.15	0.16	0.23	0.006	0.006	0.013
3‡	1	1	0.10	0.10	0.14	0.15	0.16	0.26	0.006	0.006	0.014
4	2	1	0.07	0.07	0.1	0.15	0.17	0.25	0.006	0.006	0.014
5	3	1	0.07	0.07	0.1	0.15	0.17	0.25	0.006	0.006	0.014
6	1	2	0.15	0.15	0.2	0.17	0.17	0.4	0.006	0.006	0.015
7	2	2	0.14	0.15	0.2	0.17	0.18	0.45	0.006	0.006	0.017
8	3	2	0.14	0.15	0.2	0.17	0.18	0.45	0.006	0.006	0.017
9	1	3	0.17	0.17	0.2	0.18	0.18	0.7	0.006	0.006	0.026
10	2	3	0.14	0.15	0.2	0.18	0.18	0.85	0.006	0.006	0.031
11	3	3	0.14	0.15	0.2	0.18	0.18	0.86	0.006	0.006	0.031

† In the covariance simulation for test 2, the initial estimation error for lever arm is [2 2 –2] in meters in the body frame, that is twice of the initial lever arm errors in other tests.

‡In the covariance simulation for test 3, the STD of GPS measurement noise is [0.06 0.06 0.09] in meters in the tangential frame, that is twice of the measurement noises in other tests.

Fig. 35. Test table.

Fig. 36. Test car.

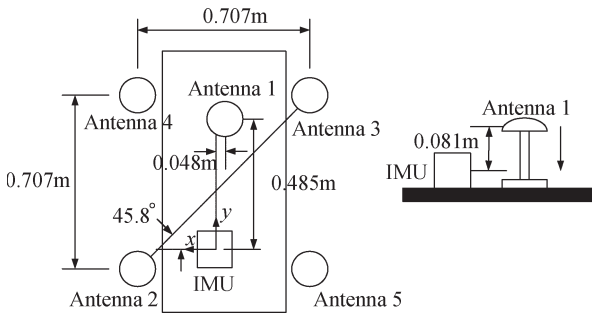

Fig. 37. Locations of sensors for the table test.

the attitude estimate, the rover attitude was measured with a multiantenna GPS attitude determination system. Its error was less than 1°. Acceleration and angular rate were measured with a very-low-grade six-degrees-of-freedom inertial measurement system. Accelerometer bias was less than 0.05 m/s^2 and the RMS of the accelerometer random noise was less than 0.01 m/s^2. Both the bias and RMS of the noise in gyro were less than 0.1 deg/s. During tests, measurement times of GPS and IMU were obtained with a counter board. The resolution of the clock counter in the counter board was 64 μs. The measurement system in this paper is similar to that in [15]. More details on it can be found in the reference.

Three tests were conducted for the estimation of the lever arm and attitude. The first test was carried out on a table. The second and third tests were carried out with a car. In each of the tests, all the sensors were mounted on a plate. The test table and test car are shown in Figs. 35 and 36, respectively. The locations of the sensors on the plates are shown in Figs. 37 and 38. The relative position and relative attitude between IMU and GPS antennas were measured with rulers and protractors before the tests were conducted. Later, these measurements were used to verify the accuracies of the estimates of the lever arm and attitude obtained from the tests.

Five GPS antennas were used in each of the tests. The one at the center or near the center of the plate was used for position measurement. The other four antennas were used for attitude measurement to examine the accuracy of attitude estimate. The four antennas formed a regular square. The length of each side of the square was $1/\sqrt{2}$ m. An IMU was also mounted on the plate. Since all the GPS antennas and inertial sensor were placed on the plate, the lever arm between the GPS antenna for position measurement and the inertial sensor could be measured to an error of less than 1 mm. The relative attitude between the inertial-sensor reference frame and the antenna-array reference frame was measured to an error of less than 1 arc min. During the tests, the computer collected measurements from GPS receivers and IMU.

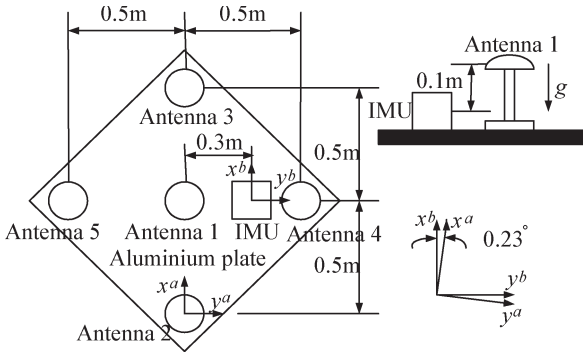

Fig. 38. Locations of sensors for car tests.

V. Test Results

In this section, test results on the estimation of lever arm and attitude were given. Measurement data from a single-antenna CDGPS and a very low-grade IMU were postprocessed to estimate navigation states. An extended Kalman filter was used to estimate lever arm, biases in IMU, and other navigation states. INS mechanization differential equations were integrated with IMU data at 134 Hz. The solution to the mechanization equations including biases of IMU was corrected at 1 Hz with GPS position measurement. Measurements from the multiantenna GPS attitude determination system were used to evaluate the accuracy of the attitude estimate.

Both the analytical and numerical simulation studies in the previous sections suggest that the estimation of navigation error states is very sensitive to maneuvering. The effect of lever-arm length on the estimates of lever arm and attitude can be negligible compared with that of maneuvering. In this section, test results are presented for three different dynamic motions with lever arms whose lengths are less than 1 m.

Considerations on a couple of tradeoffs among various factors that affect estimation performance are necessary in the tests for the estimation of lever arm and attitude. Measurements from CDGPS receivers are quite sensitive to the dynamic behavior of rover antennas [23]–[25]. Large accelerations can cause large positioning errors or loss of GPS-satellite signal tracking in severe cases. Even though large changes in acceleration and attitude are desirable for the estimation of error states, a tradeoff between measurement accuracy and the intensity of dynamic motion is necessary. The other tradeoff between the GPS-satellite geometry and the path over which the GPS rover antenna moves is also necessary. The geographic environment around the test area can significantly influence this tradeoff. A wide flat area usually has widely open sky. Thus, this type of area provides good GPS position dilution of precision (PDOP). However, a car running in this area cannot experience large changes in roll or pitch motion. On the other hand, in the area where vehicles can have large pitch or roll motions, the lines of sight between the antenna and GPS satellites can be blocked by one side of the vehicle. Even in the area where the slope of the road is not so large, the line of sight can be blocked by nearby hills, mountains, or buildings.

Experiments conducted in this paper are intended to find experimental evidence on the relationship between maneuvering and enhancement of error estimation in GPS/INS, rather than to provide best estimation results. Among tens of tests conducted on the campus, three tests that are instructive to study the effect of vehicle dynamics on the estimation of error states were introduced in this section. The first test was carried out on a table on the roof of a building in the school with widely open sky. During the table test, the plate was shaken and rolled by hand. The plate experienced mainly angular motions. The second and third tests were carried out with a car on the campus. In the car tests, the car experienced large translatory motions. The first car test was performed on a paved road on the campus. The road was on a slope and the path of the car test was selected such that the car could experience motions of full six degrees of freedom. When the car experienced relatively large accelerations, some of the GPS-satellite signals were lost temporarily during the test due to acceleration. However, as will be given later, the GPS position measurements were not degraded noticeably at these moments. The second car test was taken on an unpaved playground on the campus with widely open sky. Since the playground was unpaved, the car underwent uncomfortable vibration during the test. Because of this vibration the car experienced changes in attitude and acceleration with small magnitude persistently. In contrast to the table test, the car experienced relatively small changes in attitude rate in the car tests. Due to the small angular motion of the car, the performance of the lever-arm estimations was not satisfactory.

In order to infer the true motions of the test plate and test car, IMU measurements and the position and attitude data from GPS measurement systems were used to estimate its position, velocity, and attitude. The accuracy of the initial values of navigation states and lever arm were as follows: The lever-arm errors were less than a millimeter. The errors in the relative attitude between the reference frames of IMU and GPS antenna array were less than 1 arc min. The attitude errors of the GPS antenna array were less than 1°. The position errors were less than 2 cm. The initial velocity estimates were exact.

A. Table Test

Figs. 39–49 show the motion of the test plate. It can be seen from the figures that the test plate experienced large three-dimensional angular motions and small translatory motions. The changes in the specific force occurred mainly due to angular motions. Figs. 53–56 show estimation errors for the lever arm and attitude. In order to see the effect of the motions of the plate on the observability of the lever arm and attitude, large initial errors of these were deliberately used in the estimator. The initial error in the lever-arm estimate was 1 m in each component. The initial error in the attitude estimate was 3° for each of the roll and pitch angles. The initial error in the yaw estimate was 5°. The PDOP in Fig. 50 shows that GPS-satellite geometry was satisfactory in the table test. Figs. 51 and 52 show that GPS measurement residuals are relatively small compared with their expected STD obtained from the Kalman filter. The magnitude of the measurement residuals is less than 10 cm for the most part of the time after second 10.

Figs. 43, 44, and 53–55 show the specific force and the difference between the estimate and measurement of attitude in detail. Since translatory motions were very small, angular

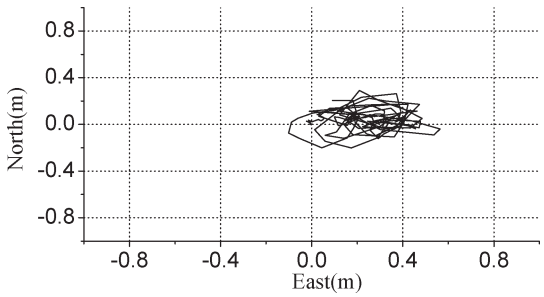

Fig. 39. Horizontal position of plate.

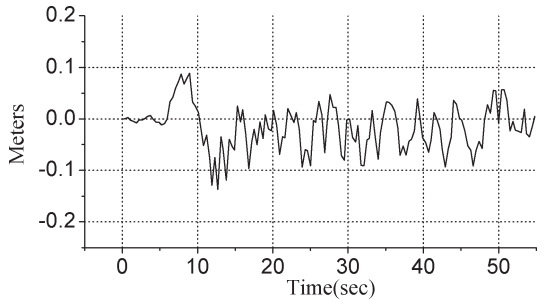

Fig. 40. Vertical position of plate.

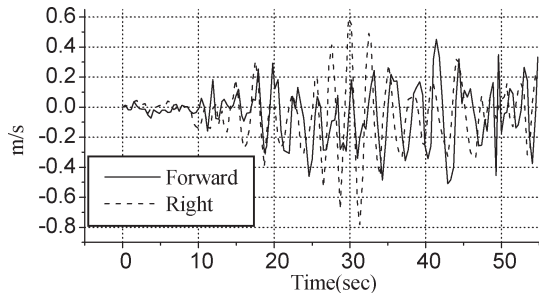

Fig. 41. Plate velocity.

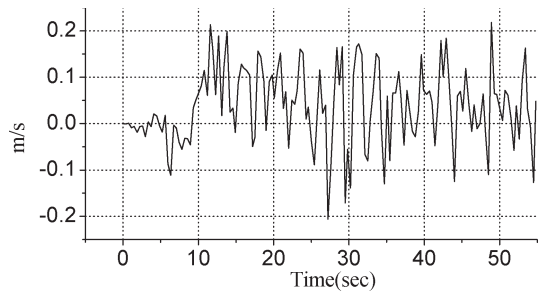

Fig. 42. Downward velocity.

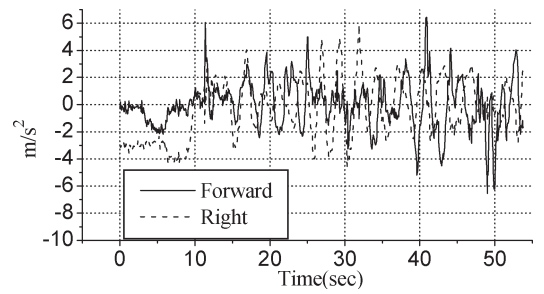

Fig. 43. Specific force.

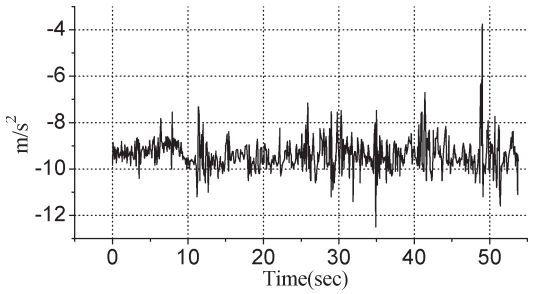

Fig. 44. Downward specific force.

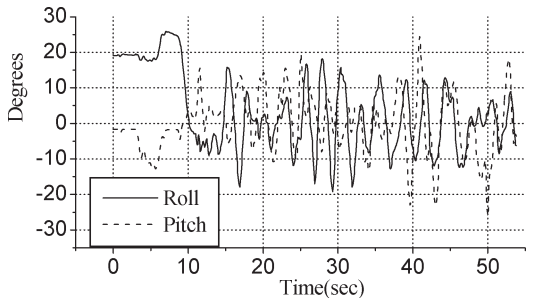

Fig. 45. Plate attitude.

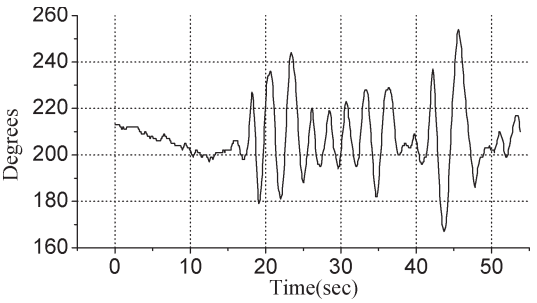

Fig. 46. Plate attitude (yaw angle).

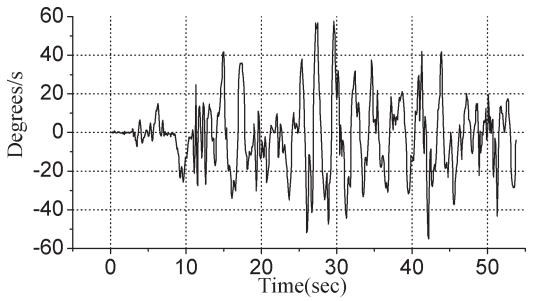

Fig. 47. Plate roll rate.

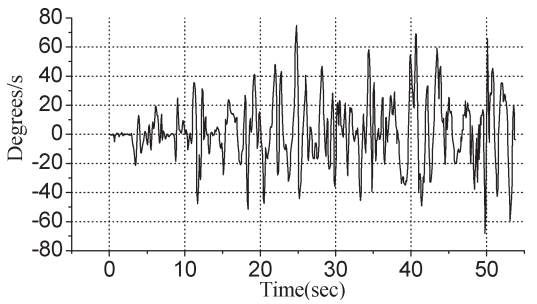

Fig. 48. Plate pitch rate.

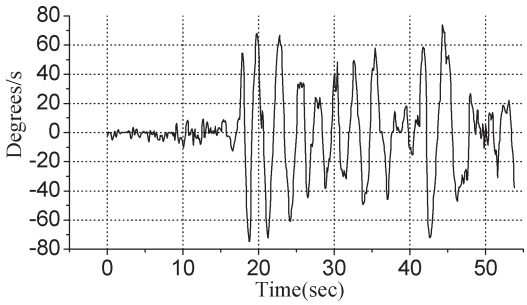

Fig. 49. Plate yaw rate.

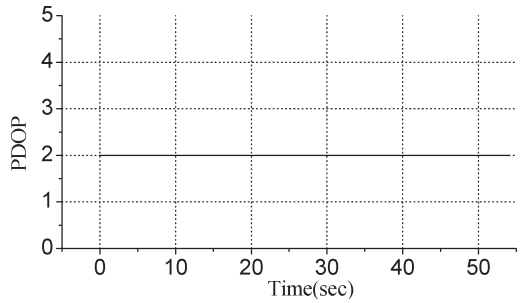

Fig. 50. GPS PDOP.

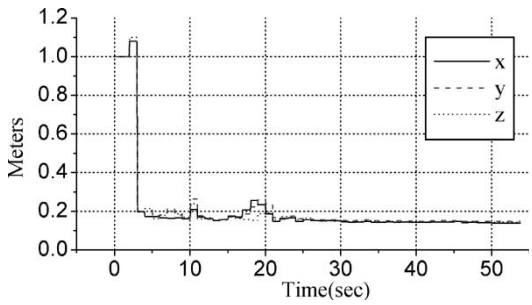

Fig. 51. STD of measurement residual obtained from the Kalman filter.

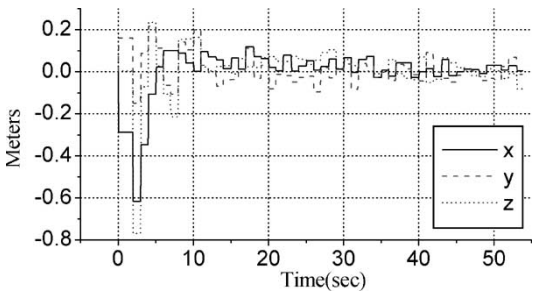

Fig. 52. GPS measurement residual.

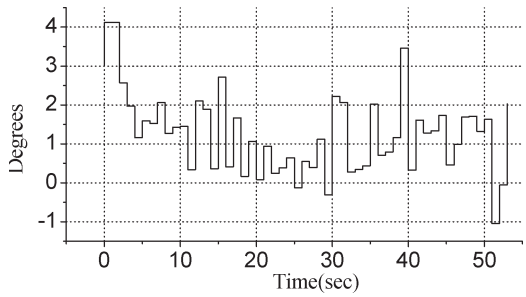

Fig. 53. Difference between the estimate and measurement of roll angle.

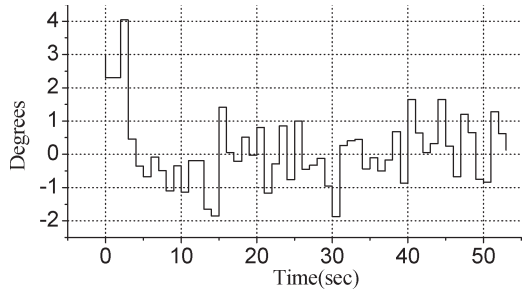

Fig. 54. Difference between the estimate and measurement of pitch angle.

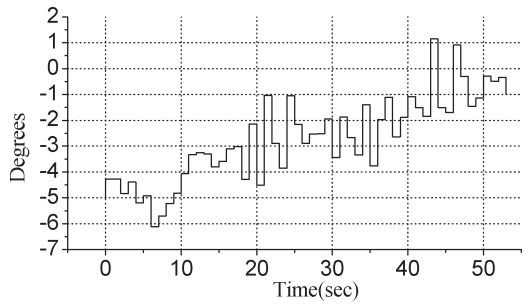

Fig. 55. Difference between the estimate and measurement of yaw angle.

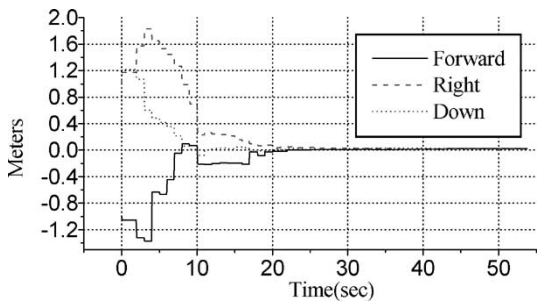

Fig. 56. Lever-arm estimation error.

motions caused the changes in the specific force. As can be seen from Figs. 43 and 45, the right-hand component of the specific force was closely related to roll angle. The figures also show a close relationship between the forward component of the specific force and pitch angle.

Errors in the estimates of roll and pitch angles reduced quickly while the plate was almost motionless in the beginning. As predicted by (6), the static errors in the horizontal components of attitude can be approximated by the ratio of accelerometer bias to the normal gravity. Yaw error in Fig. 55 is shown to decrease notably between seconds 8 and 12. Fig. 43 shows that the right-hand component of the specific force had a large variation during this time interval. Thus, it was demonstrated that the change in the horizontal component of the specific force improved the yaw estimate. However, yaw error decreases gradually at a constant rate after then. Even though test results are shown for only 55 s to improve the time resolution of the initial part of the graph, the actual test was performed over 2 min with similar motion of the test table. In the full-time processing of the test data, yaw error changed at the same rate after second 55 until the error reached $+5^{\circ}$. Thus, this decrease at a constant rate can be considered to be

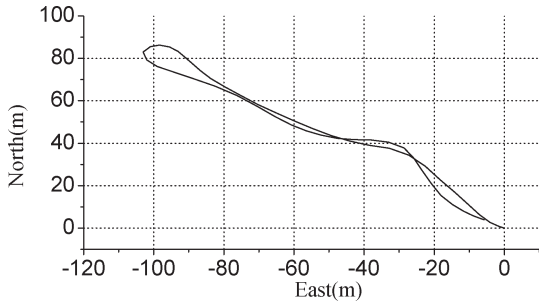

Fig. 57. Horizontal position of car.

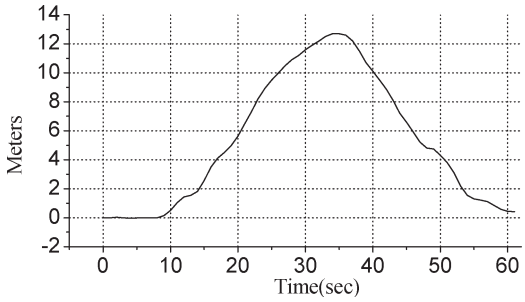

Fig. 58. Vertical position of car.

caused by gyro-bias estimation error. In contrast to the roll and pitch estimation, the yaw estimate had a relatively large error. Moreover, the error was drifting. This implied that the estimate of the vertical component of gyro bias had a large error.

A close relationship between the angular motion and lever-arm estimate can be found in the figures. Figs. 45 and 48 show that the pitch rate changed fast at around seconds 4 and 9 during the initial part of the test period. At these moments, large improvements in the forward and down components of the lever-arm error occurred, as shown in Fig. 56. Figs. 46, 49, and 56 show that when the yaw rate started to change significantly at around the second 17, forward and right-hand components of the lever-arm error reduced noticeably. Figs. 45, 47, and 56 show that roll rate and right-hand component of the lever-arm error experienced significant changes at around second 9. From these observations, it can be stated that angular motions improve lever-arm estimation. The components of the lever-arm estimation error that are orthogonal to the axis of rotation decrease during the rotational motion. The final error in the estimate of the lever arm was [3.4 1.5 2.3], in centimeters.

B. Car Test I

Figs. 57–66 show the motion of the test car. The car began to move 7 s after the start of the test. It moved in the northwest direction for about 30 s. Then, it turned 180° and returned to the initial position. The car experienced angular motions while running. The details of the car movement and errors in the estimates of the navigation states can be found in the remaining figures.

Figs. 70–72 show the differences between the attitude estimates and attitude measurements obtained from the multiantenna GPS receiver. It is shown that the GPS attitude-measurement system failed to provide measurements at

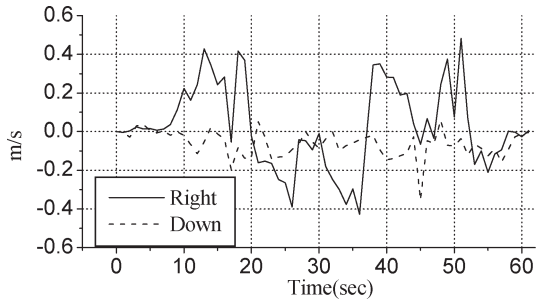

Fig. 59. Car velocity.

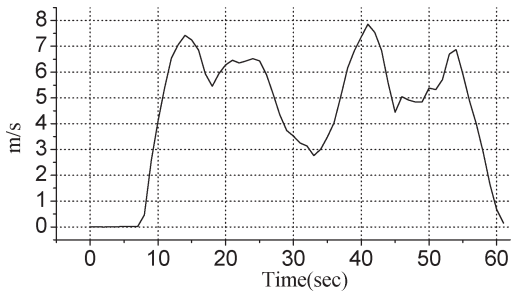

Fig. 60. Car velocity (forward).

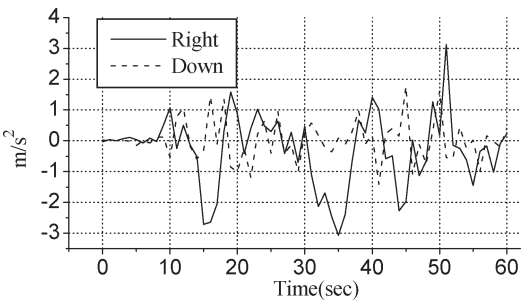

Fig. 61. Car acceleration.

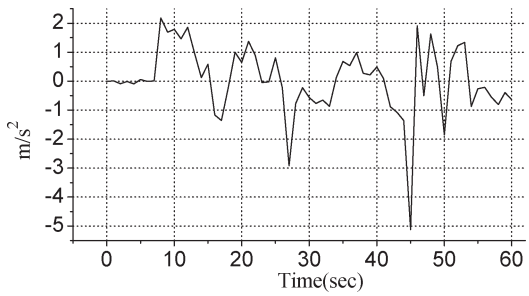

Fig. 62. Car acceleration (forward).

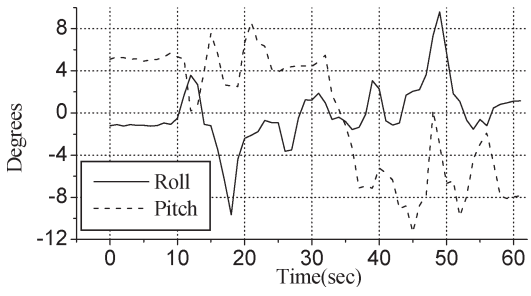

Fig. 63. Car attitude.

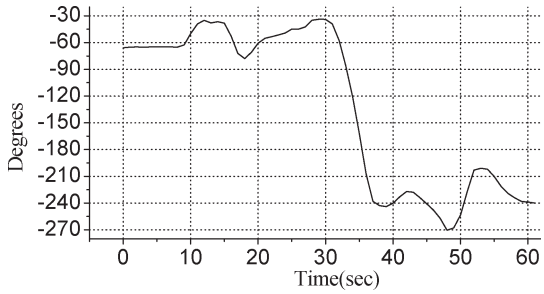

Fig. 64. Car attitude (yaw).

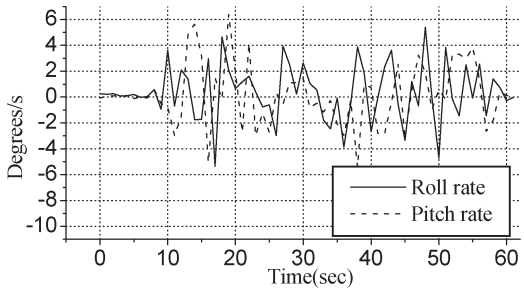

Fig. 65. Attitude rate.

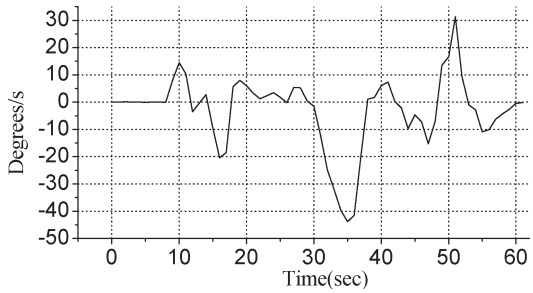

Fig. 66. Attitude rate (yaw rate).

seconds 15, 19, 52, and 53 when the car experienced large and rapid angular motions. Fig. 67 also shows that PDOP increased when yaw rate was large. These types of attitude-measurement failure and loss of GPS signal tracking also happened in other car tests in open area when the car experienced rapid and large angular motions. The reason for these attitude-measurement failures and loss of signal tracking from some of GPS satellites is thought to be the blocking of GPS signals by buildings or large acceleration during large angular motion. Even when the attitude measurements were not available, GPS position measurements were still obtained as usual. Figs. 68 and 69 show that magnitudes of the position measurement residuals are within the STD of their estimates throughout the test period. As can be expected from [24], the magnitude of measurement residuals increased when the car experienced large accelerations. Since the estimates of lever arm and attitude depended upon only position measurements, it can be inferred from the measurement residuals that the estimation results were not influenced severely by the loss of attitude measurement.

Each component of the attitude difference stayed within $\pm 2^{\circ}$ most of the time except for the initial test period and moments of bad attitude measurement. The estimation error for yaw started from 5°. Fig. 72 shows the case in which the signs of

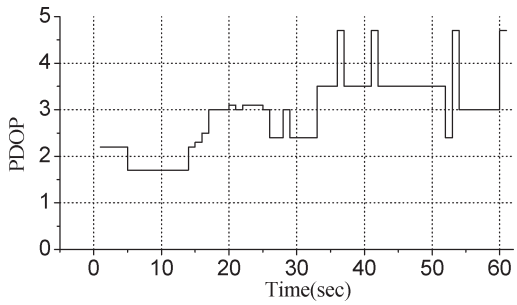

Fig. 67. GPS PDOP.

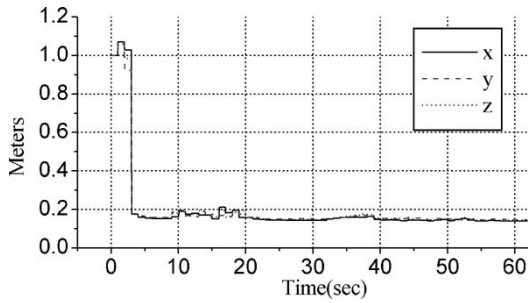

Fig. 68. STD of measurement residual obtained from the Kalman filter.

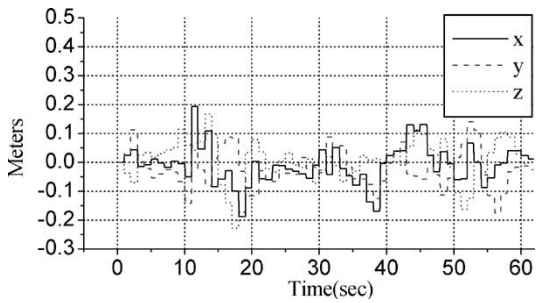

Fig. 69. GPS measurement residual.

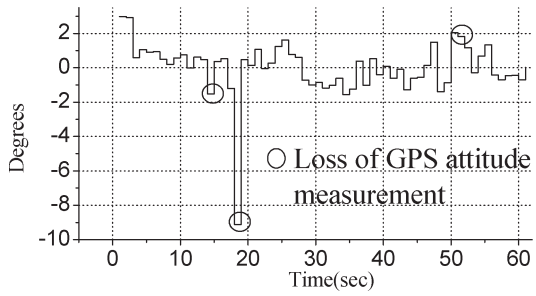

Fig. 70. Difference between the estimate and measurement of roll angle.

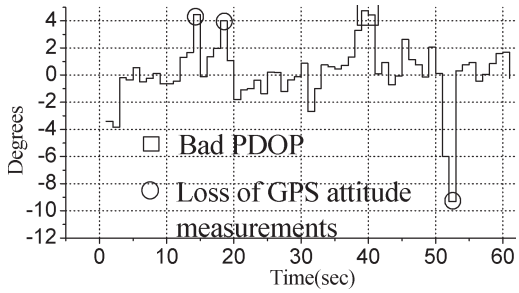

Fig. 71. Difference between the estimate and measurement of pitch angle.

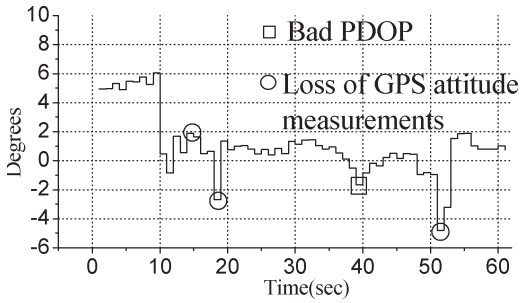

Fig. 72. Difference between the estimate and measurement of yaw angle.

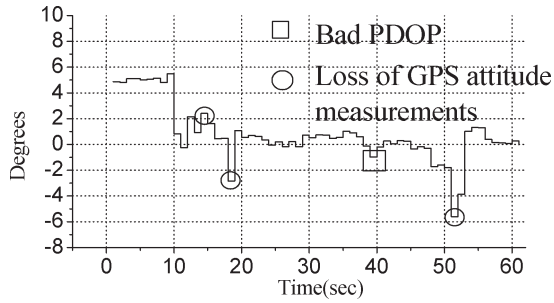

Fig. 73. Difference between the estimate and measurement of yaw angle (with initial gyro-bias correction).

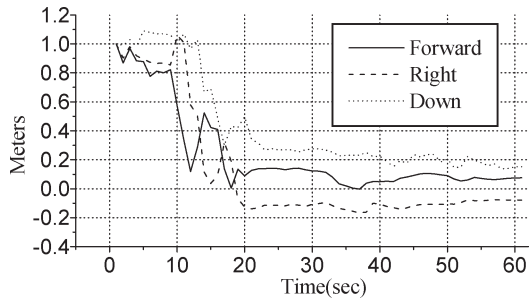

Fig. 74. Lever-arm estimation error.

the initial estimation errors of yaw angle and the downward component of gyro bias were the same. Until the moment when the car started to move, the yaw estimation error increased fast due to the large estimation error for the vertical component of gyro bias. When the car experienced forward acceleration at around second 10, it can be seen that the yaw estimation error reduced fast by a large amount. After the car experienced the forward acceleration, a noticeable increase rate of the yaw estimation error is not found in the figure, except for the periods of bad GPS attitude measurements. The estimation error for roll and pitch angles started from 3°. In Figs. 70 and 71, large improvements can be seen in the estimates of the horizontal components of attitude before the car started to move. This can be explained by the property of the estimation when the car is motionless. As given in (6), the horizontal components of the attitude estimation error are given by the ratio of the accelerometer bias to the normal gravity.

In order to verify the accuracy of the attitude estimate, the RMS of the difference between the measurement and estimate of attitude were obtained. In the calculation of the RMS value, the square of the attitude difference was summed over the time period between seconds 13 and 61, except for the abnormal moments at which GPS attitude measurement had large errors, such as seconds 14, 18, 39, 40, 51, and 52. The first 13 s were excluded because there was a large initial yaw error before second 13. The RMS values of errors in the estimates of roll, pitch, and yaw angles were 0.8°, 1.46°, and 0.8°, respectively. Noting that the GPS attitude-measurement system has subdegree error, the estimate of yaw can be considered satisfactory.

An additional estimation test is performed to observe the performance of gyro-bias estimation. In this new test, the initial estimate of gyro bias was replaced with the estimate of gyro bias obtained from the previous estimation. Except for the initial estimate of gyro bias, other initial conditions in the additional test were the same as in the first estimation. As can be seen in Figs. 72 and 73, the growth rate of the difference between the estimate and measurement of yaw between seconds 1 and 10 in Fig. 73 is smaller than that in Fig. 72. From this observation, it can be inferred that the estimate of the vertical component of gyro bias was significantly improved at the end of the first estimation.

A strong relationship between the angular motion and lever-arm estimation can be found in Figs. 63–66 and 74. The initial error in the lever-arm estimate was 1 m in each component. Figs. 64 and 66 show that large changes in yaw rate occurred between seconds 8 and 20 and between seconds 30 and 40 and at around the 50th second. It can be seen in Fig. 74 that the major reductions in the horizontal components of the lever-arm estimation error occurred during these time periods. Figs. 63 and 65 show that the car experienced noticeable rolling motions between seconds 10 and 20 and between seconds 40 and 50. During these periods, major improvements in the downward component of the lever-arm estimation error can be seen in Fig. 74.

The error in the estimate of the downward component of the lever arm was found to be relatively large compared with other components, as can be seen in Fig. 74. This might be due to insufficient roll and pitch angular motions because there were limitations on choosing the path over which the car ran.

C. Car Test II

Figs. 75–84 show the motion of the car during the second car test. The car went round an oval-shaped track. The car experienced small changes in acceleration and roll and pitch angles and large change in yaw angle. However, yaw rate was small compared with the previous tests. Figs. 85 and 86 show the difference between estimates and measurements for the attitude of the GPS antenna array. As in the previous tests, the differences for roll and pitch angles reduced quickly at the beginning and stay within 1° for most of the test time. However, the difference for yaw angle was large and greater than 2° during the final part of the test time. This implies that yaw motion and small acceleration changes are not effective in yaw-angle estimation. PDOP and measurement residuals in Figs. 87–89 show that GPS-satellite geometry and position measurement accuracy were satisfactory in this test.

Fig. 90 shows the error in the lever-arm estimate. From Figs. 82 and 84, it can be seen that significant decreases

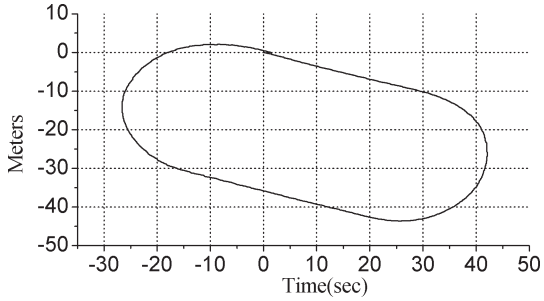

Fig. 75. Horizontal position of car.

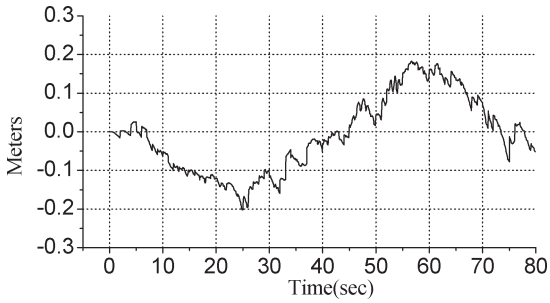

Fig. 76. Vertical position of car.

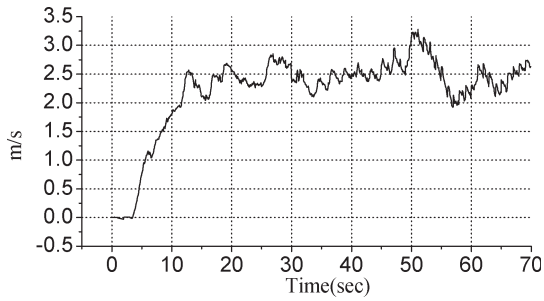

Fig. 77. Car velocity (forward).

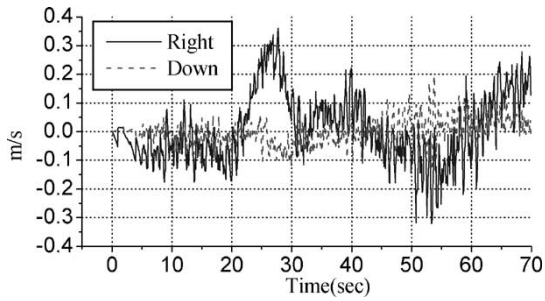

Fig. 78. Car velocity.

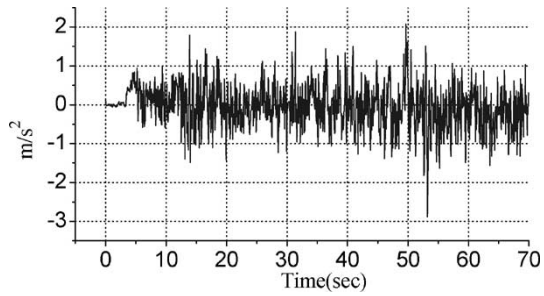

Fig. 79. Car acceleration (forward).

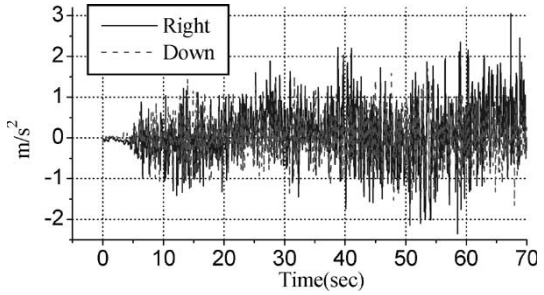

Fig. 80. Car acceleration.

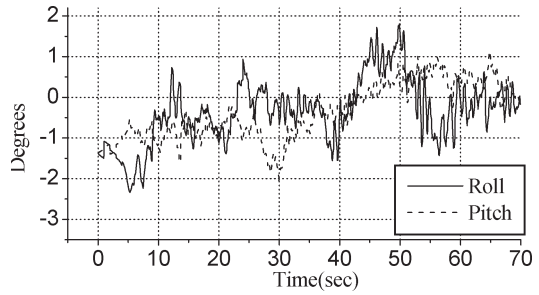

Fig. 81. Car attitude.

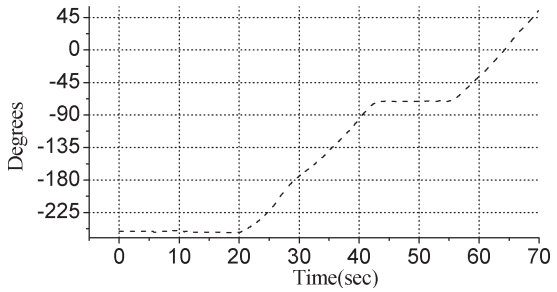

Fig. 82. Car attitude (yaw).

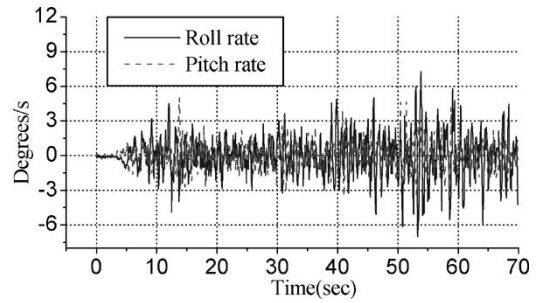

Fig. 83. Attitude rate.

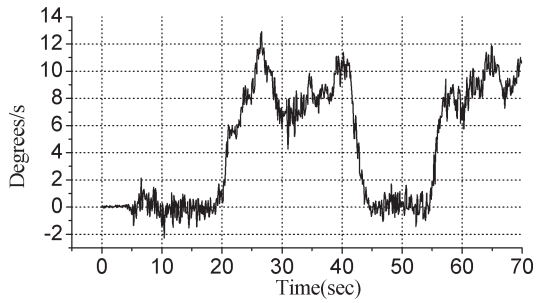

Fig. 84. Attitude rate (yaw rate).

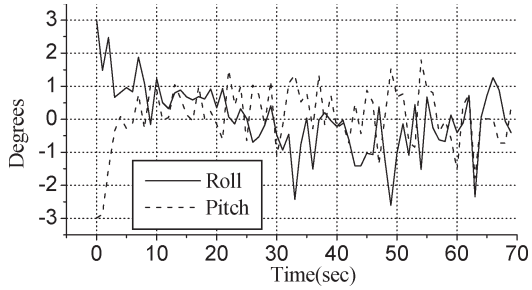

Fig. 85. Difference between the estimate and measurement of GPS antenna-array attitude.

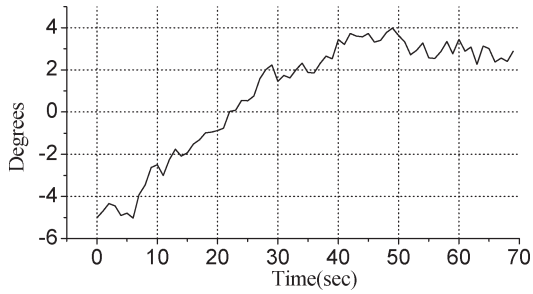

Fig. 86. Difference between the estimate and measurement of yaw angle.

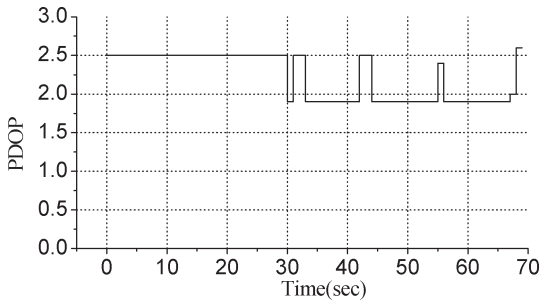

Fig. 87. GPS PDOP.

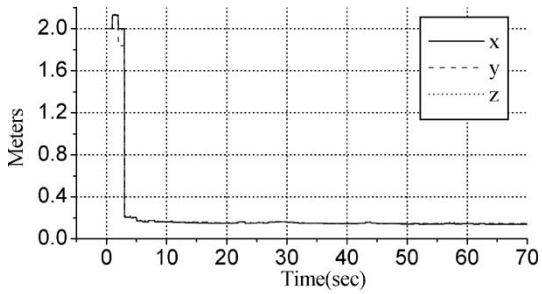

Fig. 88. STD of measurement residual obtained from the Kalman filter.

in the horizontal components of the lever-arm error occurred when yaw rate changed by a large amount. In contrast to the horizontal components, the vertical component of the lever-arm error decreased gradually during the test time. This can be explained with the horizontal components of the attitude rate in Figs. 81 and 83. Roll and pitch rates were changing persistently in small amounts all the time during the test.

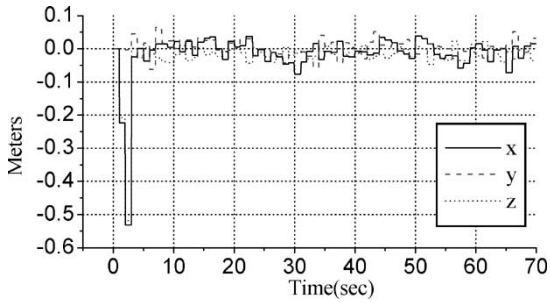

Fig. 89. GPS measurement residual.

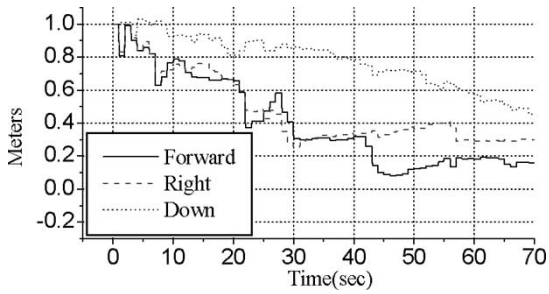

Fig. 90. Lever-arm estimation error.

TABLE II
LEVER-ARM LENGTH AND LEVER-ARM ESTIMATION ERRORS

Tests	Components	Lever arm length (mm)	Estimation error (mm)
Table test	Forward	-48	22
	Right	485	17
	Down	-81	26
Car test I	Forward	-10	73
	Right	-300	-79
	Down	-100	158
Car test II	Forward	-10	150
	Right	-300	305
	Down	-100	457

Experimental results from the table and car tests confirmed that maneuvering played an important role in the estimation of attitude and lever arm. In the table test with accompanying large changes in attitude rate, the best lever-arm estimation was obtained with centimeter-level accuracy. In the first car test in which the car experienced relatively large acceleration changes, relatively accurate yaw estimation was obtained with error less than 1°. In the second car test with relatively small changes in both acceleration and attitude rate, the worst estimates of lever arm and yaw angle were obtained. Estimation errors of lever arm in the three tests are summarized in Table II. The table shows that no explicit relationship between the estimation accuracy and the length of lever arm can be found.

The tests verify the observability analysis results in [11]: Changes in angular velocity improve lever-arm estimation and changes in acceleration improve attitude estimation. The direction of lever-arm-estimation improvement is orthogonal to the axis of rotation, and the direction of attitude improvement is orthogonal to the direction of acceleration change.

Iteratively running the Kalman filter during postprocessing of measurement data, which is a scheme introduced in [15], can be used to reduce lever-arm estimation error when angular motion could not have sufficiently fast changes during the tests as in the car tests. Details on the iterative scheme can be found in the reference.

VI. Conclusion

Both covariance simulations and experimental tests were performed on the estimation of lever arm and attitude in the integrated navigation system of a single-antenna GPS measurement system and an IMU. In the covariance simulations, the effects of vehicle maneuvering, lever-arm length, GPS measurement error, and initial estimation error on the estimation were investigated. The simulation results showed that the estimates of lever arm and attitude were very sensitive to vehicle motions. Changes in angular velocity improved the lever-arm estimation. The direction of the estimation improvement was orthogonal to the axis of rotation. Acceleration changes in the horizontal plane were also shown to improve the estimation of yaw angle. It was also shown that the estimates of lever arm and attitude were influenced noticeably by the intensity of GPS measurement noise. However, lever-arm length and initial estimation error had very small influences on the estimation when the vehicle experienced maneuvering.

Results from the experiments with the table and car confirmed that vehicle maneuverings played an important role in the estimation of lever arm and attitude. With a measurement system that consists of CDGPS and a very-low-grade IMU, a centimeter-level error in the lever-arm estimate and a subdegree error in the yaw-angle estimate were obtained from the tests.

References

[1] *Global Positioning System: Theory and Applications*, vol. II, B. W. Parkins and J. J. Spilker, Jr., Eds. Washington, DC: American Inst. Aeronaut. Astronaut., 1996.

[2] *Understanding GPS, Principles and Applications*, E. D. Kaplan, Ed. Boston, MA: Artech House, 1996.

[3] J. A. Farrell and M. Barth, *The Global Positioning System & Inertial Navigation*. New York: McGraw-Hill, 1999.

[4] K. R. Britting, *Inertial Navigation Systems Analysis*. New York: Wiley, 1971.

[5] B. M. Scherzinger, "Robust inertially-aided RTK position measurement," in *Proc. Int. Symp. Kinematic Systems Geodesy, Geomatics, and Navigation (KIS)*, Banff, AB, Canada, Jun. 2001, pp. 265–272.

[6] M. M. R. Mostafa, K. P. Schwarz and P. Gong, "GPS/INS integrated navigation system in support of digital image georeferencing," in *Proc. Institute Navigation (ION) Annu. Meeting*, Denver, CO, 1998, pp. 435–444.

[7] D. Gebre-Egziabher, R. C. Hayward, and J. D. Powell, "A low-cost GPS/Inertial attitude heading reference system (AHRS) for general aviation applications," in *Proc. IEEE Position, Location and Navigation Symp.*, Palm Springs, CA, 1998, pp. 518–525.

[8] R. R. Minor and D. W. Rowe, "Utilization of GPS/MEMS-IMU for measurement of dynamics for range testing of missiles and rockets," in *Proc. IEEE Position, Location and Navigation Symp.*, Palm Springs, CA, 1998, pp. 602–607.

[9] J. A. Farrell, T. D. Givargis, and M. J. Barth, "Real-time differential carrier phase GPS-aided INS," *IEEE Trans. Contr. Syst. Technol.*, vol. 8, no. 4, pp. 709–721, Jul. 2000.

[10] D. A. Grejner-Brzezinska, "Direct platform orientation with tightly integrated GPS/INS in airborn applications," in *Proc. Institute Navigation (ION GPS)*, Nashville, TN, Sep. 1998, pp. 885–894.

[11] S. Hong, M. H. Lee, H. H. Chun, S. H. Kwon, and J. L. Speyer, "Observability of error states in GPS/INS integration," *IEEE Trans. Veh. Technol.*, vol. 54, no. 2, pp. 731–743, Mar. 2005.

[12] S. Hong, M. H. Lee, J. A. Rios, and J. L. Speyer, "Observability analysis of INS with a GPS multi-antenna system," *Korean Soc. Mech. Eng. Int. J.*, vol. 16, no. 11, pp. 1367–1378, 2002.

[13] T. Bell, "Analysis of attitude measurement in robotic ground vehicle position determination," *Navigation*, vol. 47, no. 4, pp. 289–296, 2000–2001.

[14] S. Hong, Y. S. Chang, S. K. Ha, and M. H. Lee, "Estimation of alignment errors in GPS/INS integration," in *Proc. Institute Navigation (ION GPS)*, Portland, OR, Sep. 2002, pp. 527–534.

[15] S. Hong, M. H. Lee, S. H. Kwon, and H. H. Chun, "A car test for the estimation of GPS/INS alignment errors," *IEEE Trans. Intell. Transp. Syst.*, vol. 5, no. 3, pp. 208–218, Sep. 2004.

[16] M. K. Lee, S. Hong, M. H. Lee, S. H. Kwon, and H. H. Chun, "Observability analysis of alignment errors in GPS/INS," *J. Mech. Sci. Technol. (KSME Int. J.)*, vol. 19, no. 6, pp. 1253–1267, 2005.

[17] A. A. Sutherland, Jr., "The Kalman filter in transfer alignment of inertial guidance systems," *J. Spacecr. Rockets*, vol. 5, no. 10, pp. 1175–1180, 1968.

[18] J. Baziw and C. T. Leondes, "In-flight alignment and calibration of inertial measurement units—Part I: General formulation," *IEEE Trans. Aerosp. Electron. Syst.*, vol. AES-8, no. 1, pp. 440–449, Jul. 1972.

[19] I. Y. Bar-Itzhack and B. Porat, "Azimuth observability enhancement during inertial navigation system in-flight alignment," *J. Guid. Control*, vol. 3, no. 4, pp. 337–344, Jul./Aug. 1980.

[20] B. Porat and I. Y. Bar-Itzhack, "Effect of acceleration switching during INS in-flight alignment," *J. Guid. Control*, vol. 4, no. 4, pp. 385–389, Jul./Aug. 1981.

[21] D. Goshen-Meskin and I. Y. Bar-Itzhack, "Observability analysis of piece-wise constant systems—Part II: Application to inertial navigation in-flight alignment," *IEEE Trans. Aerosp. Electron. Syst.*, vol. 28, no. 4, pp. 1068–1075, Oct. 1992.

[22] J. F. Wagner and G. Kasties, "Improving the GPS/INS integrated system performance by increasing the distance between GPS antennas and inertial sensors," in *Proc. Nat. Technical Meeting, Institute Navigation*, San Diego, CA, Jan. 2002, pp. 103–115.

[23] M. E. Cannon, G. Lachapelle, M. C. Szarmes, J. M. Hebert, J. Keith, and S. Jokerst, "DGPS kinematic carrier phase signal simulation analysis for precise velocity and position determination," *Navigation*, vol. 44, no. 2, pp. 231–245, 1997.

[24] A. G. Evans, B. R. Hermann, B. W. Remondi, P. B. Simpson, J. L. Feist, and G. C. Wiles, "An evaluation of precise kinematic on-the-fly relative GPS positioning for a rocket sled test," in *Proc. Institute Navigation 52nd Annu. Meeting*, Cambridge, MA, Jun. 1996, pp. 71–80.

[25] D. J. Jwo, "Optimization and sensitivity analysis of GPS receiver tracking loops in dynamic environment," *Proc. Inst. Elect. Eng.—Radar Sonar Navig.*, vol. 148, no. 4, pp. 241–250, Aug. 2001.

Sinpyo Hong received the B.A. degree from Pusan National University, Busan, Korea, in 1982, the M.S. degree from Korea Advanced Institute of Science and Technology (KAIST), Seoul, Korea, in 1985, and the Ph.D. degree from the University of California, Los Angeles (UCLA), in 1993, all in mechanical engineering.

From 1985 to 1986, he was a Design Engineer at Korea Heavy Industries and Constructions Company. From 1986 to 1990, he worked as a Research Engineer for the development of a robot at Samsung Advanced Institute of Technology, Giheung, Korea. From 1993 to 1997, he was involved in the development of a navigation system for an unmanned aerial vehicle at UCLA. Since 2000, he has been working for the development of unmanned land vehicles at Pusan National University. Currently, he is a Research Professor at the Advanced Ship Engineering Research Center (ASERC), Pusan National University. His current research interests include design and analysis of integrated navigation systems and control systems.

Dr. Hong is a member of the Institute of Navigation.

Man Hyung Lee (S'79–M'83–SM'01) was born in Korea in 1946. He received the B.S. and M.S. degrees in electrical engineering from Pusan National University, Busan, Korea, in 1969 and 1971, respectively, and the Ph.D. degree in electrical and computer engineering from Oregon State University, Corvallis, in 1983.

From 1971 to 1974, he was an Instructor in the Department of Electronics Engineering, Korea Military Academy, Seoul, Korea. He was an Assistant Professor with the Department of Mechanical Engineering, Pusan National University, from 1974 to 1978. From 1978 to 1983, he held positions as a Teaching Assistant, Research Assistant, and Postdoctoral Fellow at Oregon State University. Since 1983, he has been a Professor in the College of Engineering, Pusan National University, where he was a Pohang Iron and Steel Company, Pohang, Korea (POSCO) Chair Professor in the School of Mechanical Engineering from 1997 to 2003 and was Dean of the College of Engineering, Pusan National University, from March 2002 to February 2004. His research interests are estimation, identification, stochastic processes, bilinear systems, mechatronics, micromachine automation, and robotics. He is the author of more than 750 technical papers.

Dr. Lee was Program Chair of the 1998 4th ICASE Annual Conference. He was a General Cochairman of the 2001 IEEE International Symposium on Industrial Electronics (ISIE) and is a General Cochairman of the 30th Annual Conference of the IEEE Industrial Electronics Society (IECON '04). He is a member of the American Society of Mechanical Engineers, the Society for Industrial and Applied Mathematics, and the Society of Photo-Optical Instrumentation Engineers.

Ho-Hwan Chun received the B.Sc. and M.Sc. degrees in ship and ocean engineering from Pusan National University, Busan, Korea, in 1983 and 1985, respectively. In 1988, he received the Ph.D. degree in naval architecture from Glasgow University, Glasgow, U.K.

He worked as a Yard Research Fellow at Glasgow University from 1988 to 1990 and as a Principal Researcher at Hyundai Maritime Research Institute, Ulsan, Korea, from 1991 to 1993. Since 1994, he has served as a Professor in the Department of Naval Architecture and Ocean Engineering, Pusan National University. In 2002, he became the Director of Advanced Ship Engineering Research Center (ASERC), designated by the Ministry of Science and Technology (MOST) Korea. His main research area is hydrodynamics such as hull-form design, hull and structure interactions with waves, wing in ground-effect (WIG) and drag reduction, etc.

Sun-Hong Kwon received the B.S. degree in naval architecture from Pusan National University, Busan, Korea, in 1978, the M.E. degree in ocean engineering from Stevens Institute of Technology, Hoboken, NJ, in 1983, and the Ph.D. degree in aerospace and ocean engineering from Virginia Polytechnic Institute and State University, Blacksburg, in 1986.

Since 1986, he has been with Pusan National University as a Faculty Member in the Department of Naval Architecture and Ocean Engineering. His current research interests are the application of wavelet analysis to ocean engineering and development of a sea-wave monitoring system by using radar images.

Jason L. Speyer (M'71–SM'82–F'85–LF'05) received the S.B. degree in aeronautics and astronautics from the Massachusetts Institute of Technology, Cambridge, in 1960 and the Ph.D. degree in applied mathematics from Harvard University, Cambridge, in 1968.

His industrial experience includes research at Boeing, Raytheon, Analytical Mechanics Associated, and the Charles Draper Laboratory. He was the Harry H. Power Professor in Aerospace Engineering at the University of Texas, Austin, and is currently a Professor in the Mechanical and Aerospace Engineering Department at the University of California, Los Angeles (UCLA). He spent a research leave as a Lady Davis Visiting Professor at the Technion, Israel Institute of Technology, Haifa, Israel, in 1983 and was the 1990 Jerome C. Hunsaker Visiting Professor of aeronautics and astronautics at the Massachusetts Institute of Technology.

Dr. Speyer has twice been an elected member of the Board of Governors of the IEEE Control Systems Society. He has served as an Associate Editor of the IEEE TRANSACTIONS ON AUTOMATIC CONTROL and as Chairman of the Technical Committee on Aerospace Control. He is a Fellow of the American Institute of Aeronautics and Astronautics. From October 1987 to October 1991 and from October 1997 to October 2001, he served as a member of the United States Air Force (USAF) Scientific Advisory Board. He received the Mechanics and Control of Flight Award and Dryden Lectureship in Research from the American Institute of Aeronautics and Astronautics in 1985 and 1995, respectively. He was awarded the Air Force Exceptional Civilian Decoration in 1991 and 2001 and the IEEE Third Millennium Medal in 2000.